Microhardness and wear behaviour of surface modified Ti6Al4V/Zr-TiC metal matrix composite for advanced material

A.P. I. POPOOLA[a*], O. F. OCHONOGOR[a], M. ABDULWAHAB[a], S. PITYANA[a, b], C. MEACOCK[b]
[a]*Department of Chemical and Metallurgical Engineering, Faculty of Engineering and the Built Environment, Tshwane University of Technology, P.M.B. X680, Pretoria, South Africa 0001*
[b]*Council for Scientific and Industrial Research, National Laser Centre, Pretoria, South Africa*

Surface modification of titanium alloy (Ti-6Al-4V) was made using a Rofin Sinar 4 kW Nd: YAG laser. A laser multi-track 50% overlapping process was employed to produce Zr and Zr-TiC metal matrix composite (MMC) coatings on Ti6Al4V substrate. The beam diameter was set at 4 mm. The microstructures of fabricated composites consist of homogeneous distribution of TiC particles which were free of cracks with x-ray diffraction (XRD) analyses indicating formation of interstitial carbides. Multilayer cladding involving Ti6Al4V + (100%Zr and Ti6Al4V + (Zr+TiC) MMCs fabricated with 10, 20, 30 and 40 %TiC were developed. Multiple track deposited samples revealed microhardness improvement as high as 1048.7 HV for 60%Zr+40%TiC MMC and the least hardness displayed is 606.6 HV for 90%Zr+10%TiC MMC. The wear result showed that the developed MMCs have low wear rate as compared to the substrate.

(Received April 27, 2012; accepted October 30, 2012)

Keywords: Laser cladding, metal matrix composites, Ti6Al4V, rapid solidification, interstitial carbides, Biomedical

1. Introduction

Titanium and its alloys have found major applications in industries such as aerospace, electronics, biomedical materials, energy and defence due to their high performance and etc [1-10]. However, based on some industrial and specific service requirements where abrasive, wear, erosion and corrosion properties are needed, the alloy is still considered to exhibit poor wear and corrosion resistance. Hence, surface modification to enhance the limiting properties of this alloy is necessary. Laser surface alloying (LSA) have been reported [11-12] to be a promising technique for the surface improvement of the alloy because of the advantages derived over other rapid solidification methods. The use of lasers for the surface modification of titanium and its alloys have equally been widely studied and reported [3,4,6,13-20]. In titanium, alloying elements tend to stabilize either the low temperature, close-packed hexagonal alpha phase, or the high-temperature allotrope, body-centred cubic beta phase. To fully optimize the mechanical properties, titanium alloys are worked to control the microstructure. Microstructure plays a vital role in the determination of mechanical properties of an alloy [21]. Ti-6Al-4V is an alloy whose microstructure depends strongly upon chemical composition. Hence the control of microstructure is necessary to improve the physical and mechanical properties of Ti-6Al-4V [22]. Safdar et al. [23] studied the evaluation of microstructural development in electron beam melted Ti-6Al-4V. They reported that the microstructures of Ti-6Al-4V consist of columnar grains of prior β phase growing along the built direction. LSA often creates thermal distortions which result in severe residual stresses. Laser surface cladding overcomes some of these obstacles since only a thin surface layer of the substrate melts during the process and combines with the additive materials to form the coatings [24].

Laser cladding is an economical and highly flexible surface modification method in the aero-engine industry [14] and provides a promising manufacturing method to build up three dimensional dense metallic components directly from computer-aided design (CAD) files [25]. MMCs reinforced with hard ceramic particles have received great attention because they offer superior strength, stiffness, and good wear resistance compared to their monolithic counterparts [26]. Titanium-titanium carbide alloy is a promising material for high performance engineering systems given the ability to form carbide metal composite with well refined microstructure consisting of hard titanium particle metal matrix [27]. Generally, it is widely acceptable that carbides exhibit the required combination of high hardness, low toughness and good wear resistance. Zirconium alloy is similar to titanium in that it is considered a reactive metal reason being that it displays a high affinity for oxygen as well [28]. A unique characteristic of this material is that it is biocompatible, which means that for people who have nickel allergies and cannot have knee implants made of cobalt chromium alloy as a result of nickel being included naturally in the cobalt chromium alloy; this provides an alternative. The use of zirconium alloy in new ceramic knee implants completely eliminates the risk of nickel-allergy [29]. When zirconium is heated, it oxidizes on the surface, thus producing zirconium oxide on the surface which is self-healing and shields the substrate metal from chemical attack up to certain temperature [29]. In the

present study, an attempt has been made to surface-clad Zr and Zr+TiC powders on Ti-6Al-4V titanium alloy using laser surface cladding technique with the aim of enhancing the hardness and wear resistance of the substrate suitable for biomedical applications.

2. Experimental procedure

2.1 Laser Cladding Process

The laser cladding system was used to deposit different compositions of reinforcement ranging from 100%Zr, 90%Zr+10%TiC, 80%Zr+20%TiC, 70%Zr+30%TiC clad material on the substrate (Ti6Al4V) to form metal matrix composites with different relative volume fractions. The substrate was sand blasted before laser treatment. The process was facilitated by using flow from two powder feed hoppers containing Zr and TiC particles combined to generate a powder stream of the required relative volume fractions and morphology. The beam diameter was 4 mm. Spheroidal gas atomised Zr powder particles with a size distribution of 32-120 μm and TiC particles with a size distribution of 32-45 μm with an irregular morphology were used. The parameters relevant to this measurement are shown in Table 1.

Table 1: Laser cladding processing parameters (multi-track process with 50% overlap and beam diameter at 4 mm).

S/N	Laser Power (W)	Scan Speed (mm/s)	Powder Feed Rate (g/min) (Zr) 32-120 μm	Powder Feed Rate (g/min) (TiC) 32-45 μm	Powder mixtures
1	750	10	2.5	0.0	100%Zr
2	750	10	2.2	0.3	90%Zr + 10%TiC
3	750	10	1.9	0.6	80%Zr + 20%TiC
4	750	10	1.6	0.9	70%Zr + 30%TiC
5	750	10	1.3	1.2	60%Zr + 40%TiC

2.2 Materials Characterization

After laser cladding process was completed, the samples were cut cross sectionally with a Struers Discotom-2 cutting machine. Careful surface preparations were carried out and followed systematically in order to reveal the important details of the microstructure. The chemical reaction and surface adhesion between zirconium and other reinforcement mixtures led to the formation of an improved and new structure in the matrix. The following characterization tests were carried out: X-ray diffraction (XRD) analyses of the powders and the MMCs using a Philips PW 1713 X-ray diffractometer fitted with a monochromatic Cu Kα radiation set at 40 kV and 20 mA was used to determine the phase composition of powder. Phase identification was done using Philips Analytical X'PertHighScore® software with an in-built International Centre for Diffraction Data (ICSD) database. The polished cross sectional surfaces of MMCs as well as the worn surfaces from wear test were analyzed using a Joel scanning electron microscope (SEM) Model JSM-6510 equipped with energy dispersive spectrometer (EDS). While elemental composition was determined by EDS analysis.

2.3 Hardness and Abrasive Wear Test

Microhardness measurement was done on the cross-sectional surface of the samples using a Dura Scan Vickers hardness tester. Indentations started from the surface of the clad layers through to the base. The Vickers microhardness of the samples was determined with 100 μm spacing between corresponding indentations using a load of 100 g for 15 s dwell time.

The MMC samples of 65 x 25 x 10 mm diameters were tested using the well-known dry abrasion rubber wheel tester. Three body abrasive wear tests were performed on an ASTM-G65-04 dry sand rubber wheel apparatus. Silica sand of particle size distribution between 300-600 microns was used as the abrasive material. The sample was mounted firmly in the sample holder and pressed against the rim of the rubber wheel with the desired normal force. The dry silica sand with particle size distribution ranging from 300-600 microns was allowed to fall freely between the wheel and the sample. The flow rate was set to 7.89 g/s. An applied load of 30 N was used. Each sample was abraded for 30 minutes to evaluate the mass loss. For each sample two specimens were used and the average mass loss per 30 minutes was used to determine the mass loss. The morphology of the worn surface was examined using SEM/EDS analysis.

3. Result and discussions

3.1 Characterization of substrate and developed MMCs

Fig. 1 shows the micrograph of substrate with the EDS; the EDS revealed the Ti and Al elements present in the substrate which are the major constituents.

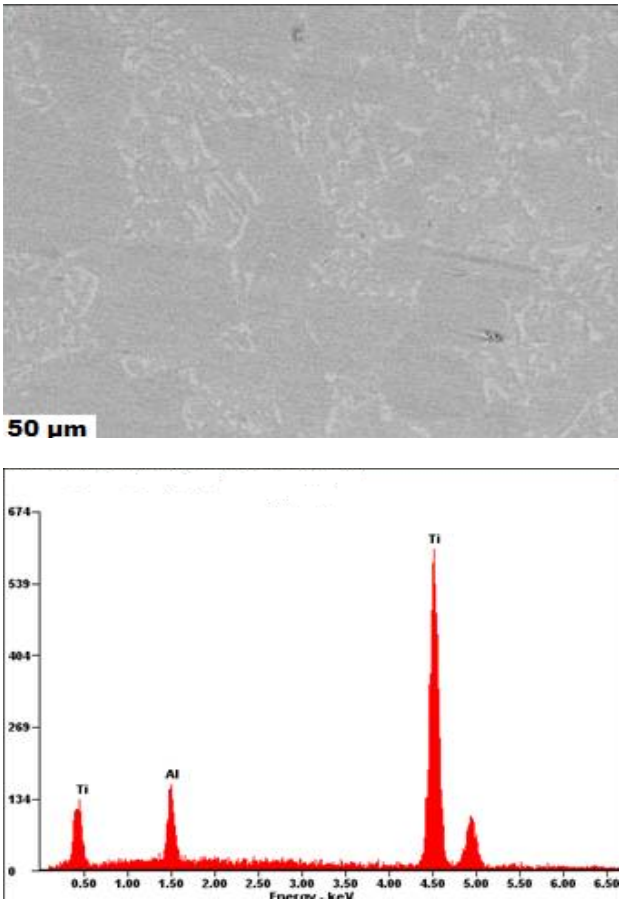

Fig. 1. SEM micrograph of substrate (as-received) with the EDS.

The SEM micrographs showing the overview of some cladded samples can be seen in Figure 2; a) 100%Zr (Sample 1) b) 60%Zr+40%TiC (Sample 5). An obvious change in the morphology as a result of increases in the TiC particles was noticed in Figure 3, where all the samples SEM micrographs are display. EDS indicated that the dark spots are titanium particles, while the grey regions are the Zr particles which have higher percentage out of the two reinforcement powders employed. From Figure 3e, the homogeneous distribution of the Zr and TiC particles on the 60%Zr+40%TiC MMC can be seen. From the clad zone mainly, the Zr was found staying at the background while the Ti particles stayed locked up within the Zr background, this can be seen in Fig. 3.

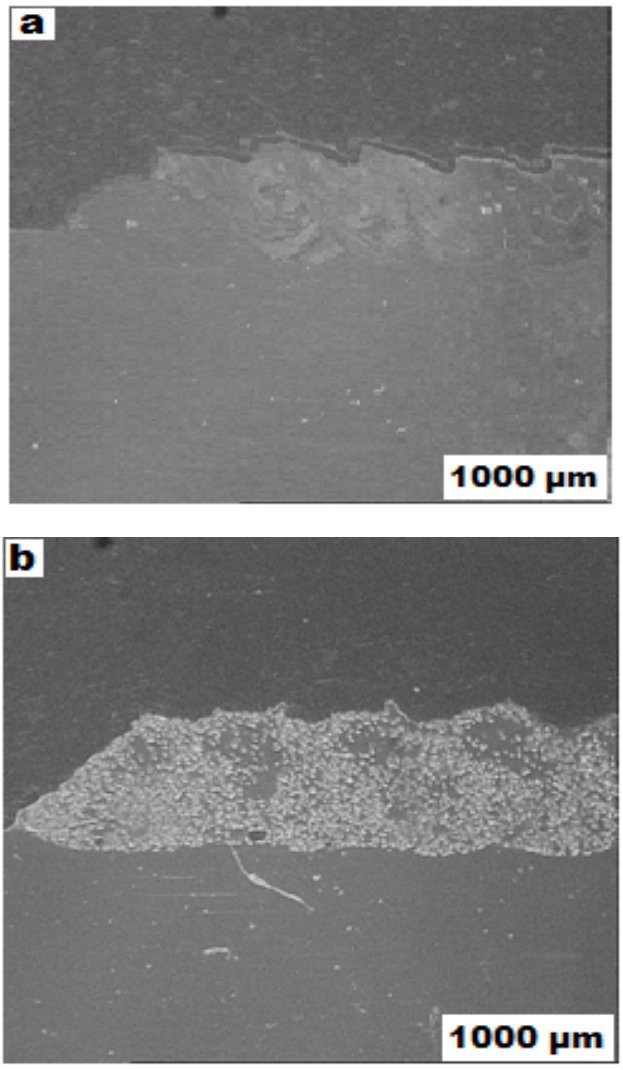

Fig. 2. SEM micrographs showing the overview of the MMCs; a) 100% Zr and b) 60%Zr+40%TiC MMC.

It can be seen from Fig. 3 that the dark spots (Ti particles) on the micrographs increases with the Ti reinforcement proportion used for cladding.

XRD spectra of the substrate and MMCs are shown in Figure 4. In general, the XRD analysis indicate the presence of Zr, ZrC, and TiC for all the composites fabricated except for the 100%Zr MMC. The formation of interstitial carbides which are very hard phases ZrC and TiC were evident from XRD result.

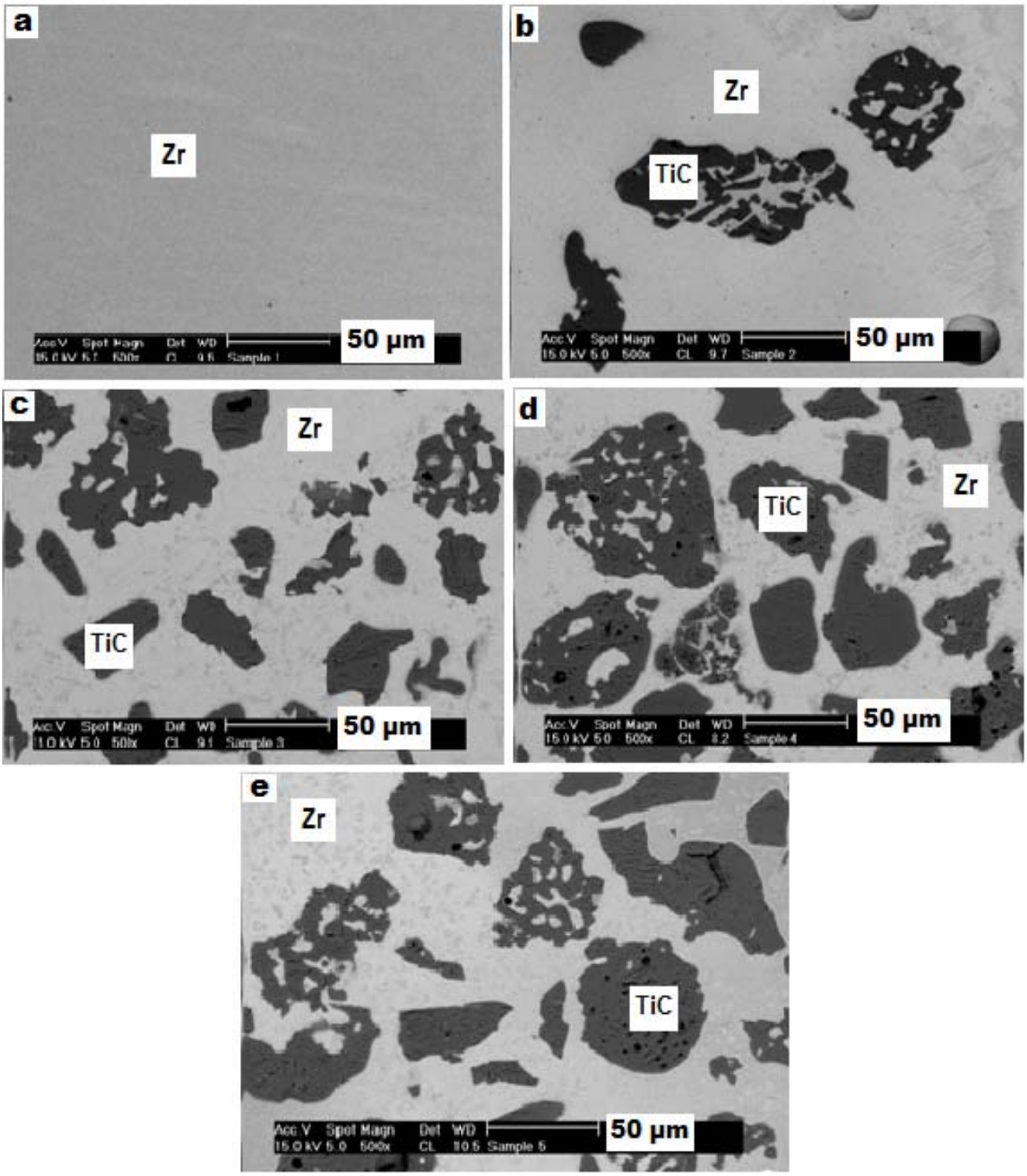

Fig. 3. SEM macrographs showing multiple layer laser clad samples; a) 100%Zr b) 90%Zr+10%TiC c) 80%Zr+20%TiC d) 70%Zr+30%TiC and e) 60%Zr+40%TiC.

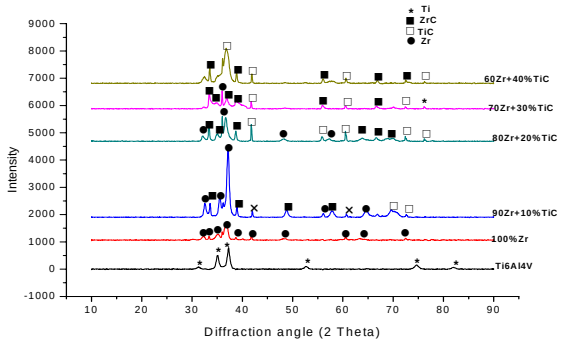

Fig. 4. XRD pattern of Ti–6Al–4V (Substrate), 100%Zr, 90%Zr+10%TiC, 80%Zr+20%TiC, 70%Zr+30%TiC and 60%Zr+40%TiC samples.

3.2 Microhardness Variation in Developed MMCs

Fig. 5 shows the average hardness variation of MMCs with different composition of admixture powders. Experimental result indicated that the hardness of the MMCs increases with an increase in the ceramic powder content (see Fig. 5).

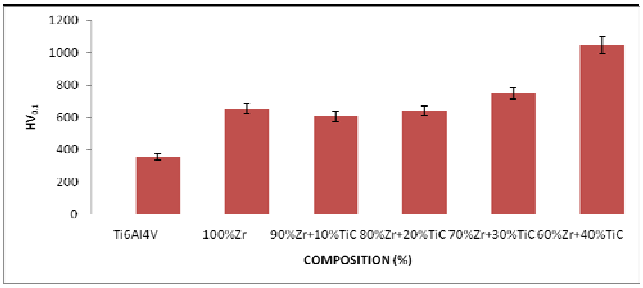

Fig. 5: Variation of average hardness of laser multilayer MMCs with reinforcement composition.

The built height is the height of the irregularities with respect to a reference line or clad height, Figure 6 revealed that highest built height of 1346.77 µm was obtained for the MMC with highest hardness value. The initial hardness of the substrate was about 357.3 $HV_{0.1}$.

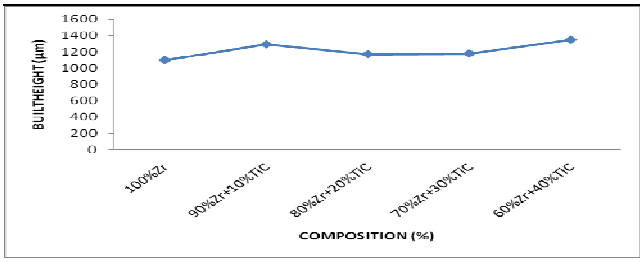

Fig. 6. Variation of built height of Zr-TiC MMCs with reinforcement compositions.

There was a near-linear increase in the hardness value with increasing TiC ceramic content, reaching a peak hardness of 1048.7 $HV_{0.1}$ for the 60%Zr+40%TiC MMC and 640.1 $HV_{0.1}$ for the 80%Zr+20%TiC MMC. Similar improvement was recorded [11, 29]. The microhardness value of 90%Zr+10%TiC MMC was lower (606.6 $HV_{0.1}$) as compared with 100%Zr (653.1 $HV_{0.1}$) after which it increased with TiC composition. This occurrence might likely be associated with the trace of porosity found on 90%Zr+10%TiC MMC. On a general note, porosity free MMCs were obtained for all samples, which account for the improvement in the hardness value with increase in the ceramic powder content. In particular, the EDS of the MMC with highest hardness, shows evidence of some elements such as Ti, C and Zr.

3.3 Wear behaviour of the MMCs

The results of the wear test and the built height for the MMCs are presented in Table 2. The variation of the mass loss with composition of MMCs can be found in Figure 7 with their respective SEM micrographs after wear test in Fig. 8.

Table 2: Experimental data for abrasive wear test.

S/N	Composition (%)	Mass loss (wt. %)	Phases Present	Built height (µm)
1	100%Zr	0.017	Zr	1096.77
2	90%Zr+10%TiC	0.005	Zr, TiC	1290.32
3	80%Zr+20%TiC	0.004	Zr, TiC	1169.35
4	70%Zr+30%TiC	0.006	Zr, TiC	1177.42
5	60%Zr+40%TiC	0.011	Zr, TiC	1346.77
6	Substrate (Ti–6Al–4V)	0.106	Ti, Al, V	_____

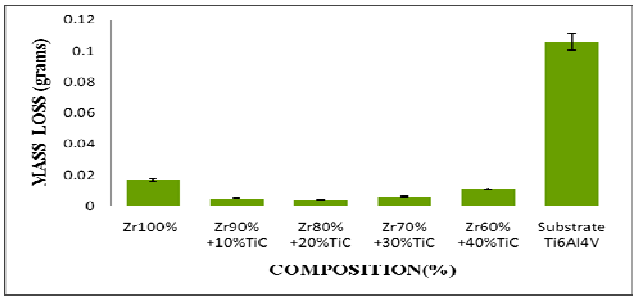

Fig. 7. Variation of abrasive mass loss with Zr and TiC compositions.

The cumulative wear resistance of the MMCs did not increase with increase in the ceramic content the way the hardness values increased; which then means there is no correlation between the hardness and wear properties of the MMCs developed. 80%Zr+20%TiC MMC exhibited the best wear resistance amongst the developed MMCs. The result further showed that the abrasive mass loss for the substrate was the highest which was expected. The improved wear resistance in laser clad surfaces is attributed to the higher hardness displayed by the clad surfaces due to the effects of the laser cladding process; grain refinement resulting from the effect of laser beam and the presence of TiC, ZrC and ZrCZr hard phases precipitated in the Ti-matrix.

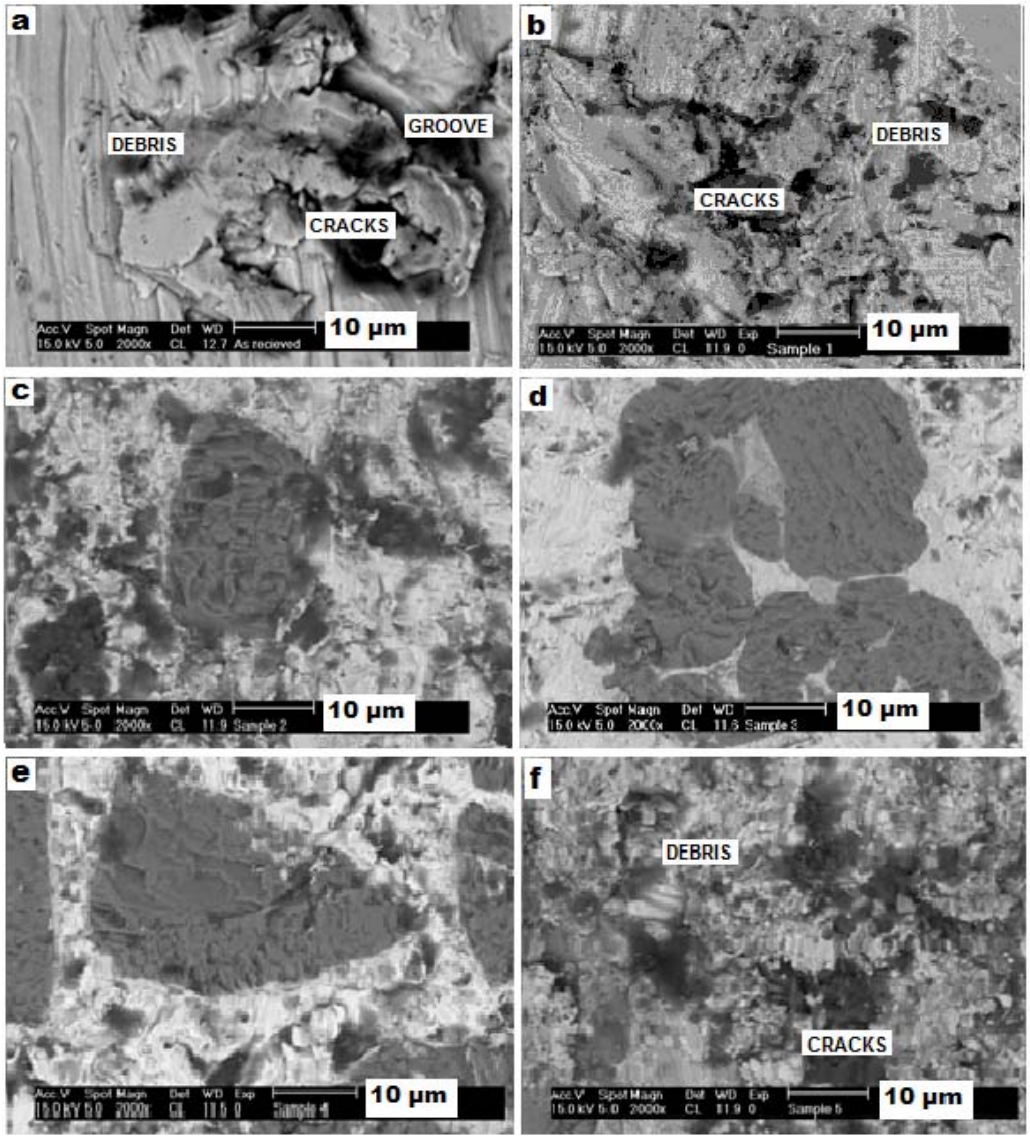

Fig. 8. SEM images of wear scars of the substrate (as received) as well as the MMCs; a) substrate b) 100%Zr c) 90%Zr+10%TiC d) 80%Zr+20%TiC e) 70%Zr+30%TiC and f) 60%Zr+40%TiC.

Generally, the mass loss of the MMCs decreased with an increase in the TiC composition and a decreasing Zr content. From SEM micrograph of the substrate, the mechanism of wear was by selective removal of Ti6Al4V, presence of deep scratches, delamination of materials from the surface, evidence of pits and worn out debris. This micrograph also indicates massive damaged regions caused by plastic deformation and fatigue due to the

repeated action of the abrasive particle sand. In addition, evidence of deep grooves and fracture was observed on the micrograph. The 100%Zr MMC revealed similar damaged regions on the worn surface of the MMC. This sample however exhibited better wear resistance than the substrate in that the damages observed were not as much as seen on the as received sample. However the Zr-TiC MMCs show lesser degree of deformation generally, worn surfaces consist predominantly of fine scratches. The 60%Zr+40%TiC MMC despite the high percentage of TiC and the highest hardness value displayed by this sample did not display best wear resistance, because grooves and debris can be found on its surface, this can however be attributed to perfect surface homogeneity displayed by this sample, surface inhomogeneity has been reported to favour wear resistance. The mechanism of wear can be said to be combination of adhesive and majorly abrasive for the as received sample. The mechanism of wear for the MMCs was by mild abrasive with the inclusion of silica sand on the worn surfaces.

4. Conclusions

SEM micrographs of the laser clad 90%Zr+10%TiC MMC showed little porosity, but no evidence of porosity found on 60%Zr+40%TiC MMC and low levels of variation in the cladded geometry. Microstructure showed a fine crystal grains distribution in the titanium alloy matrix.

The microhardness values of the composites increases with increasing addition of ceramic reinforcement. The microhardness of the clad zone improved to about 1048.7 $HV_{0.1}$ for the MMCs reinforced with 60%Zr+40%TiC due to the formation of interstitial carbides (TiC, ZrC).

Improved hardness led to increased wear resistance of the developed metal matrix composites. The wear resistance of the laser clad surfaces were enhanced significantly for all the MMCs with wear mechanism being majorly abrasive.

Acknowledgements

This material is based upon work supported financially by the National Research Foundation. The National Laser Centre, CSIR, Pretoria is appreciated for laser facility.

References

[1] H. Nasin-Abarbekoh, A. Ekrami, A. A. Ziaei-Moayyed, Mater. Des., **37**, 223 (2012)
[2] D.S. Milovanovic, B.B. Radaka, B.M. Gakovic, D. Batani, M.D. Momcilovic, M.S. Trtica, J Alloys Compd., **501**, 89 (2010).
[3] R. Filip, J Achiev Mater. Sci. Manuf. Eng., **15**, 174 (2006).
[4] M. Das, S. Bysakh, D. Basu, T.S.S. Kumar, V.K. Balla, S. Bose, A. Bandyopadhyay. Surf. Coat. Techn., **205**, 4366 (2011).
[5] R. Rocha, Braz Dent. J, **17**(1), 20 (2006).
[6] Z.D. Liu, X.C. Zhang, F.Z. Xuan, Z.D. Wang, S.T. Tu, Mater. Des., **37** 268 (2012).
[7] Y.S. Tain, L.X. Chen, C.Z. Chen, Cryst. Growth Des., **6**(6) 1509 (2006).
[8] P. Jiang, X.L. He, X.X Li, L.G. Yu, H.M. Wang, Surf. Coat. Techn., **130** 24 (2000).
[9] W. Pang, H.C. Man, T.M. Yue, Mater. Sci. Eng. A **390** 144 (2005).
[10] J. Fornell, S. Gonzalez, E. Pellicer, N.V. Steenberge, P. Perez, S. Surinach, M.D. Baro, J. Sort,. J Alloy Compd., article in-press, dol:10.1016/j.jallcom.2011.10.057, 2011.
[11] Y.S. Tian, C.Z. Chen, S.T. Li, Q.H. Huo, Applied Surface Science, **242** 177 (2005).
[12] Y. Chuang, S. Lee, H. Lin, Mater. Trans., **47**(1) 106 (2006).
[13] J.H. Abboud, D.R.F. West, J Mater. Sci .Letters, **9** 308 (1990).
[14] K.H. Richter, S. Orban, S. Nowotny, Laser cladding of the titanium alloy Ti6242 to restore damaged blades. Proceedings of the 23th International Congress on Applications of Lasers and Electro-Optics, 2004.
[15] V.M. Fedirko, I.M. Pohrelyuk, O.M. Yas'kiv, Mater. Sci., **42(**3) 299 (2006).
[16] V.M. Fedirko, A.T. Pichuhin, O.H. Luk'yanenko, V.S. Onuferko, Mater. Sci., **41**(2) 208 (2005).
[17] A.L. Gavze, A.P. Matevos'yan, A.V. Nesterovich, B.Y. Bogdanovich, Metal Sci. Heat Treat, **43**(9-10) 363 (2001).
[18] A.L. Gavze, I.I. Shestakov, Metal Sci. and Heat Treatment, **48**(5-6) 252 (2006).
[19] I.M. Pohrelyuk, V.M. Fedirko, T.M. Kravchshyn, Mater. Sci., **43(**6) 807 (2007).
[20] A. Lisiecki, A. Klimpel, Arch. Mater. Sci. Eng., **31**(1) 53 (2008).
[21] R. Dinga, Z.X. Guo, A. Wilson, Mater Sci Eng A **327** 233- (2002).
[22] L. Zenga, T.R. Bieler, Mater. Sci. Eng. A **392** 403 (2005).
[23] A. Safdar, L.Y. Wei, A. Snis, Z. Lai, Mater. Charact., **65** 8 (2012).
[24] Y. Pei, J.T.M.D. Hosson, An OIM study of five-fold branched Si particles produced by laser cladding of an Al-Si alloy. Silicon particles: Application note-EBSD, AMETEK, www.edax.com, 2002.
[25] D. Liu, S.Q. Zhang, A. Li, H.M. Wang, J Alloys Compd., **496** 189 (2010).
[26] J.D. Majumdar, B.R. Chandra, A.K. Nath, I. Manna, J Mater. Proc. Techn., **203,** 505 (2008).
[27] A.P.I. Popoola, D.I. Adebiyi, Scientific Research and Essays, **6**(29) 6104 (2011).
[28] Y. Chen, H.M. Wang, J Alloys Compd., **351** 304 (2003).
[29] J.R. Davis. Materials for Medical Device, 48(2003).

*Corresponding author: popoolaapi@tut.ac.za